Genomics Proteomics Bioinformatics 19 (2021) 123–139

Genomics Proteomics Bioinformatics

www.elsevier.com/locate/gpb
www.sciencedirect.com

ORIGINAL RESEARCH

Gigantic Genomes Provide Empirical Tests of Transposable Element Dynamics Models

**Jie Wang [1,*], Michael W. Itgen [2], Huiju Wang [3], Yuzhou Gong [1], Jianping Jiang [1]
Jiatang Li [1], Cheng Sun [4], Stanley K. Sessions [5], Rachel Lockridge Mueller [2,*]**

[1] *CAS Key Laboratory of Mountain Ecological Restoration and Bioresource Utilization & Ecological Restoration and Biodiversity Conservation Key Laboratory of Sichuan Province, Chengdu Institute of Biology, Chinese Academy of Sciences, Chengdu 610041, China*
[2] *Department of Biology, Colorado State University, Fort Collins, CO 80523, USA*
[3] *School of Information and Safety Engineering, Zhongnan University of Economics and Law, Wuhan 430073, China*
[4] *Institute of Apicultural Research, Chinese Academy of Agricultural Sciences, Beijing 100093, China*
[5] *Biology Department, Hartwick College, Oneonta, NY 13820, USA*

Received 25 March 2020; revised 29 November 2020; accepted 30 November 2020
Available online 4 March 2021

Handled by Ting Wang

KEYWORDS

TE expression;
TE diversity index;
Genome size evolution;
Caecilian;
Transposon ecology

Abstract Transposable elements (TEs) are a major determinant of eukaryotic **genome size**. The collective properties of a genomic TE community reveal the history of TE/host evolutionary dynamics and impact present-day host structure and function, from genome to organism levels. In rare cases, TE community/genome size has greatly expanded in animals, associated with increased cell size and changes to anatomy and physiology. Here, we characterize the TE landscape of the genome and transcriptome in an amphibian with a giant genome — the **caecilian** *Ichthyophis bannanicus*, which we show has a genome size of 12.2 Gb. Amphibians are an important model system because the clade includes independent cases of genomic gigantism. The *I. bannanicus* genome differs compositionally from other giant amphibian genomes, but shares a low rate of ectopic recombination-mediated deletion. We examine TE activity using expression and divergence plots; TEs account for 15% of somatic transcription, and most superfamilies appear active. We quantify TE diversity in the caecilian, as well as other vertebrates with a range of genome sizes, using diversity indices commonly applied in community ecology. We synthesize previous models that integrate TE abundance, diversity, and activity, and test whether the caecilian meets model predictions for genomes with high TE abundance. We propose thorough, consistent characterization of TEs to strengthen future comparative analyses. Such analyses will ultimately be required to reveal whether

[*] Corresponding authors.
E-mail: wangjie@cib.ac.cn (Wang J), rlm@colostate.edu (Mueller RL).

Peer review under responsibility of Beijing Institute of Genomics, Chinese Academy of Sciences / China National Center for Bioinformation and Genetics Society of China.

https://doi.org/10.1016/j.gpb.2020.11.005
1672-0229

the divergent TE assemblages found across convergent gigantic genomes reflect fundamental shared features of TE/host genome evolutionary dynamics.

Introduction

Transposable elements (TEs) are segments of DNA that move within genomes [1]. Because their movement is often associated with an increase in copy number, these elements constitute a substantial but variable fraction of eukaryotic genomes, such as 2.7% in pufferfish (*Takifugu rubripes*) [2] and 85% in maize (*Zea mays*) [3]. TEs were discovered by Barbara McClintock in the late 1940s, demonstrating that genomes are far more dynamic entities than previously thought [4].

Although they share the characteristic of intra-genomic mobility, TEs are highly diverse sequences. TE classification has been updated over the years to reflect new discoveries [5]. Several classification systems have been proposed that establish groups according to transposition mechanism, structure, sequence similarity, and shared evolutionary history [6–10]. These classification systems have allowed the community of genome biologists to annotate TEs in the genomes of diverse species, identifying differences in overall TE composition, TE activity, TE turnover dynamics, and TE domestication across the tree of life [11–13].

Overall TE content is the main predictor of haploid genome size, which shapes a variety of traits including the sizes of nuclei and cells, the rates of development and basal metabolism, and the structural complexity of organs [14–21]. TE load is shaped by mutation (specifically the insertion of new TE sequences by transposition and their removal by deletion), selection (which targets individual TE loci as well as the pathways that control TE activity) [22], and genetic drift (which affects how efficiently purifying selection removes harmful TE sequences) [23]. How these forces interact to generate genome size diversity across the tree of life remains incompletely understood. Groups of related species that vary in TE load and genome size provide critical model systems for studying this fundamental question [24].

Across animals, genomic gigantism is rare. Within vertebrates, it is best understood in the salamanders (order Caudata), a clade of ~700 species of amphibians with haploid genome sizes that range from 14 Gb to 120 Gb [25]. Fossil cell size data demonstrate that salamander genome sizes have been large for ~160 million years [26]. Comparative genomic analyses demonstrate that salamander genomes have high levels of TEs, particularly long terminal repeat (LTR) retrotransposons, and that these high levels reflect low rates of DNA loss in non-LTR retrotransposons, low rates of ectopic recombination-mediated LTR retrotransposon deletion, and PIWI-interacting RNA (piRNA)-mediated TE silencing machinery that includes relatively few TE-targeting piRNAs [27–33]. Phylogenetic comparative analyses demonstrate that salamanders' enormous genomes result from an abrupt change in evolutionary dynamics at the base of the clade, implying a discrete shift in the balance among the evolutionary forces shaping TE accumulation [34,35].

In addition to salamanders, there are two other living clades of amphibians: caecilians (order Gymnophiona), and frogs and toads (order Anura). Caudata and Anura are sister taxa, and Gymnophiona is the sister taxon to Caudata + Anura. Frogs and toads are a well-studied group of 7175 species. Of the 278 species (in 78 genera) for which genome size estimates exist, a handful of species in three different genera have genomes that reach or exceed 10 Gb [25], providing independent examples of genomic expansion. Genomic data examined to date show diverse TE landscapes across species [36–41], but no sequence data exist (to our knowledge) for those with the largest genomes. Caecilians are a relatively understudied group of 214 species, all of which are limbless, serpentine, burrowing or aquatic animals with reduced eyes, ringed bodies, and strong, heavily ossified skulls. Genome size estimates exist for roughly 20 species and range from 2.8 Gb to 13.7 Gb [25,35]. These data show yet another independent example of genomic expansion within amphibians, suggesting a clade-wide propensity towards TE accumulation. Genomic data for caecilians are sparse, but growing based on successes of the G10K consortium and others [42,43]. Published data are lacking for species with the largest genomes. This lack of amphibian data underlies a major gap in our knowledge of vertebrate genome evolution [13]. More generally, a lack of detailed information on TE biology in large and repetitive genomes, reflecting persistent assembly and annotation challenges, underlies a major gap in genome biology as a whole.

In this study, we present an analysis of TE biology in *Ichthyophis bannanicus* (Gymnophiona: Ichthyophiidae), a caecilian with a large genome, which we show has a genome size of 12.2 Gb. We compare the caecilian to other vertebrates with diverse genome sizes, demonstrating how the TE community in a large genome can be used to evaluate existing models of TE dynamics. *I. bannanicus* is a relatively small species (adult size 30–41 cm) with an aquatic larval stage and a terrestrial/fossorial adult stage. Its distribution includes China and northern Vietnam, and it is an IUCN species of Least Concern. We analyze both genomic shotgun sequence data and RNA-seq data from diverse tissues to answer the following specific questions: 1) What abundance and diversity of TEs make up the large *I. bannanicus* genome? 2) What are the amplification and deletion dynamics of TEs in the genome? 3) What contribution does the large genomic TE load make to the somatic transcriptome? 4) Do the patterns of genomic TE composition and overall TE expression fit the predictions of models of TE dynamics in large genomes? We show that up to 68% of the *I. bannanicus* genome is composed of TEs, with another 9% identified as repetitive sequences not classifiable as known TEs. The two most abundant TE superfamilies, DIRS/*DIRS* and LINE/*Jockey*, account for ~ 50% of the genome. Unlike salamander genomes, the *I. bannanicus* genome has relatively few LTR retrotransposons, demonstrating that repeated instances of extreme TE accumulation in amphibians do not reflect failure to control a specific type of TE. We show that the rate of ectopic recombination-mediated deletion is lower in *I. bannanicus* than in vertebrates with more typical genome sizes, and that TE expression is high. We quantify and compare TE diversity in *I. bannanicus* and ten other vertebrates using indices common in community ecology. We demonstrate that comparative analyses of TE diversity can be a powerful tool for evaluating models of TE dynamics, and we show that it could be even more powerful if researchers adopt a uniform approach to TE diversity analysis. We propose such an approach to move the field forward. Taken together, our results demonstrate that computationally feasible analyses of large genomes can reveal the genomic characteristics favoring expanded TE communities, as well as the resulting impact of high TE load on the transcriptome. Such analyses targeting phylogenetically diverse organisms can yield fundamental insights into the complex ways in which TEs drive genome biology.

Results

The *I. bannanicus* genome is 12.2 Gb and contains most known TE superfamilies

The haploid genome size of *I. bannanicus* was estimated to be 12.2 Gb based on analyses of Feulgen-stained erythrocytes following established methods [14]. This estimate is similar to the other published estimate from the same genus (*I. glutinosus*, 11.5 Gb) [35]. We used the PiRATE pipeline [44], designed to mine and classify repeats from low-coverage genomic shotgun data in taxa that lack genomic resources. The pipeline yielded 59,825 contigs (**Table 1**). RepeatMasker mined the majority of the repeats (37,123 out of 59,825; 62.1%). dnaPipeTE was the second most effective tool, mining 19,160 repeats (32.0%), followed by RepeatScout (3.0%) and TE-HMMER (2.7%). In this pipeline, TEdenovo, LTRharvest, HelSearch, SINE-Finder, and MITE-Hunter found few additional repeats, and we found no additional repeats using MGEScan-non-LTR. Clustering with CD-HIT-est at a 95% sequence identity cutoff yielded 51,862 contigs, and clustering at 80% yielded 23,092 contigs.

Repeat contigs were annotated as TEs to the levels of order and superfamily in Wicker's hierarchical classification system [7], modified to include several recently discovered TE superfamilies, using PASTEC [45]. Of the 59,825 identified repeat contigs, 50,471 (84.4%) were classified as known TEs (**Table 2**). TEs representing eight of the nine orders proposed in Wicker's system are present in the *I. bannanicus* genome; only Crypton was not identified by our pipeline (although we note that 192 chimeric contigs were filtered out that included a Crypton annotation, and 9 transcriptome contigs were annotated as Crypton). Within these eight orders, our analyses identified 25 TE superfamilies, each represented by 2–26,507 annotated contigs. Non-autonomous TRIM and LARD elements, as well as MITE elements, are also present in the *I. bannanicus* genome, represented by 229, 28, and 146 contigs, respectively, and an additional 277 contigs were only annotated to the level of order or class (*i.e.*, unknown LINE, SINE, and TIR or unknown Class I) (Table 2).

Table 1 Repeat contigs identified by different methods/software of the PiRATE pipeline

TE-mining method	Software	No. of repeats clustered at 100% identify
Similarity-based	RepeatMasker	37,123 (62.1%)
	TE-HMMER	1585 (2.7%)
Structure-based	HelSearch	17 (0.0%)
	LTRharvest	23 (0.0%)
	MGEScan-non-LTR	0
	MITE-Hunter	12 (0.0%)
	SINE-Finder	17 (0.0%)
Repetitiveness-based	TEdenovo	102 (0.2%)
	RepeatScout	1786 (3.0%)
Repeat-building-based	dnaPipeTE	19,160 (32.0%)
In total		59,825 (100%)

Note: TE, transposable element.

78% of the *I. bannanicus* genome is repetitive, dominated by DIRS/*DIRS* elements

To calculate the percentage of the caecilian genome composed of different TEs, the shotgun reads were masked with RepeatMasker v-4.0.7 using our caecilian-derived repeat library. We then repeated the RepeatMasker analysis excluding the unknown repeats and compared the two sets of results. This comparison provided a rough approximation of the number of unknown repeat contigs that were TE-derived sequences that were divergent, fragmented, or otherwise unidentifiable by our pipeline. 68.20% of these sequences (measured as bp) were masked as repetitive when the repeat library included only the 50,471 contigs classified as TEs and the 29 contigs annotated as putative multi-copy host genes: 66.10% were identifiable to the superfamily level of TEs (Table 2), an additional 1.94% were identifiable only to the class or order level, and 0.17% were multi-copy host genes. When the analysis was performed including the 9325 unknown-repeat contigs, along with the classified TEs and putative multi-copy host genes, 77.62% of the data were masked as repetitive overall, suggesting that the unknown repeats comprise 9.42% of the genome. However, the percentage of the genome identified as known TEs decreased from 68.04% to 54.72% with the inclusion of unknown repeats, demonstrating that many reads were sufficiently similar to known TEs to be masked by them when unknown repeat contigs were not available as a best-match option. This result suggests that at least some of the unknown repeats are TE-derived sequences.

Class I TEs (retrotransposons) make up 52.09%–63.68% (unknown repeats included or excluded in the repeat library, respectively) of the *I. bannanicus* genome; they are almost 20 times more abundant than Class II TEs (DNA transposons; 2.63%–4.36%). DIRS/*DIRS* is the most abundant superfamily (25.88%–30.20% of the genome), followed by LINE/*Jockey* (16.92%–20.59%), LINE/*L1* (3.05%–3.23%), LTR/*ERV* (1.62%–1.82%), LINE/*RTE* (1.50%–1.60%), and LTR/*Gypsy* (1.10%–1.35%); all are retrotransposons (Table 2). TIR/*hAT* (0.57%–1.15%), TIR/*CACTA* (0.52%–0.56%), and TIR/*Tc1–Mariner* (0.49%–0.59%) are the most abundant superfamilies of DNA transposons (Table 2). These proportions differ from those found in the gigantic genomes of salamanders, where LTR/*Gypsy* elements dominate (7%–20% of the genome, depending on species), DIRS/*DIRS* elements never exceed 7% of the genome, and LINE/*Jockey* elements never exceed 0.03% of the genome [30,32]. Here and throughout the paper, we are interpreting our results based on the assumption that the genomic shotgun data are a random representation of the whole genome; Illumina reads should sample the genome in a random and independent manner, despite some stochastic sampling error.

Table 2 Classification of repeat contigs and summary of repeats detected in the genome and somatic transcriptome

Order	Superfamily	Percent of genome (%)	No. of genomic contigs (100% identical)	No. of genomic contigs (95% identical)	No. of genomic contigs (80% identical)	Average genomic contig length (100% identical) (bp)	Longest genomic contig (bp)	No. of transcriptome contigs (100% identical)	No. of transcriptome contigs (80% identical)	Total expression (summed TPM)	Average expression (Min, Max)
Class I – Retrotransposon – Autonomous											
LTR	*ERV*	1.62–1.82	1578	1132	376	548	10,231	1894	559	5564.35	2.94 (0.03, 239.46)
	Gypsy	1.10–1.35	1324	1159	523	665	5544	1080	662	1441.05	1.33 (0.01, 17.75)
	Retrovirus	0.01	13	13	9	591	1198	19	15	19.76	1.04 (0.12, 4.25)
	Bel–Pao	0.00	3	3	3	407	541	5	5	3.46	0.69 (0.33, 1.05)
	Copia	0.00	2	2	2	222	297	124	99	117.54	0.95 (0.08, 5.93)
DIRS	*DIRS*	25.88–30.20	26,507	23,221	8513	346	4452	25,426	12,652	68,259.45	2.68 (0.01, 476.25)
	Ngaro	0.46–0.47	988	954	411	488	1975	674	455	983.7	1.46 (0.02, 10.81)
PLE	*Penelope*	0.19–0.22	542	540	469	226	1686	1649	1454	2728.03	1.65 (0.04, 71.46)
LINE	*Jockey*	16.92–20.59	12,004	10,490	2911	350	3609	14,267	6613	34,709.94	2.43 (0.01, 172.77)
	L1	3.05–3.23	4139	3962	1867	738	5045	4736	3533	7277.91	1.54 (0.01, 166.70)
	RTE	1.50–1.60	1020	883	130	269	2717	863	356	3412.23	3.95 (0.01, 124.43)
	R2	0.12–0.22	51	48	20	290	1011	243	110	550.38	2.26 (0.02, 16.34)
	I		-	-	-	-	-	2	2	3.93	1.97 (0.75, 3.18)
	Unknown LINE	0.03	5	-	3	807	1743	-	-	-	-
Class I – Retrotransposon – Non-autonomous											
SINE	*7SL*	0.09	123	108	47	263	1030	-	-	-	-
	5S	0.02	25	25	14	194	1384	64	59	156.72	2.45 (0.29, 13.91)
	tRNA	0.00	11	11	5	158	294	208	193	539.05	2.59 (0.17, 49.49)
	Unknown SINE	0.55–1.66	203	146	41	235	498	484	370	2509.77	5.19 (0.06, 371.09)
Retrotransposon derivative	TRIM	0.44–1.78	229	159	53	432	3226	601	301	1759.19	2.93 (0.10, 33.17)
	LARD	0.10–0.19	28	18	5	1928	10,505	4	1	39.14	9.79 (0.69, 32.83)
Unknown Class I		0.03–0.19	61	58	55	261	1259	-	-	-	-

(*continued on next page*)

Table 2 Classification of repeat contigs and summary of repeats detected in the genome and somatic transcriptome

Order	Superfamily	Percent of genome (%)	No. of genomic contigs (100% identical)	No. of genomic contigs (95% identical)	No. of genomic contigs (80% identical)	Average genomic contig length (100% identical) (bp)	Longest genomic contig (bp)	No. of transcriptome contigs (100% identical)	No. of transcriptome contigs (80% identical)	Total expression (summed TPM)	Average expression (Min, Max)
Class II – DNA transposon – Subclass 1											
TIR	*hAT*	0.57–1.15	338	263	155	425	2589	309	182	565.60	1.83 (0.04, 31.47)
	CACTA	0.52–0.56	135	92	46	444	1734	277	111	1179.55	4.26 (0.11, 143.05)
	Tc1–Mariner	0.49–0.59	548	438	189	370	2028	1180	421	4312.73	3.65 (0.01, 93.19)
	PIF–Harbinger	0.41–0.45	373	262	115	386	1951	113	69	189.23	1.67 (0.11, 12.58)
	piggyBac	0.06–0.08	25	20	16	880	2521	87	35	200.72	2.31 (0.07, 22.85)
	Sola	0.01	12	11	7	608	2150	11	5	9.72	0.88 (0.17, 2.22)
	Mutator/MuDR	0.00	2	2	2	321	380	18	15	22.5	1.25 (0.22, 4.33)
	P	0.00	2	2	1	237	250	2	2	3.27	1.64 (1.40, 1.87)
	Zisupton		-	-	-	-	-	7	2	16.9	2.41 (0.43, 11.13)
	Kolobok		-	-	-	-	-	7	5	7.75	1.11 (0.25, 2.68)
	Academ		-	-	-	-	-	4	3	18.0	4.50 (1.45, 11.95)
	Unknown TIR	0.04–0.05	8	7	5	307	621	-	-	-	-
Crypton	*Crypton*		-	-	-	-	-	9	3	6.34	0.70 (0.05, 3.57)
Transposon derivative	MITE	0.50–1.42	146	134	82	199	577	1297	1028	3480.60	2.68 (0.01, 72.2)
Class II – DNA transposon – Subclass 2											
Maverick	*Maverick*	0.04–0.05	24	22	12	1037	5305	80	31	122.99	1.54 (0.06, 6.87)
Helitron	*Helitron*	0.00	2	2	2	298	352	20	13	65.84	3.29 (0.05, 14.14)
Total		54.72–68.04	50,471	44,187	16,089	395.4	10,505	55,764	29,364	140277.34	2.52 (0.01, 476.25)

Note: For "percent of genome (%)", the first number is estimated including unknown repeats from the repeat library, and the second number is estimated excluding unknown repeats. TPM, transcripts per million; LTR, long terminal repeat; DIRS, *Dictyostelium* intermediate repeat sequence; PLE, Penelope; LINE, long interspersed nuclear element; SINE, short interspersed nuclear element; TIR, terminal inverted repeat.

The *I. bannanicus* genome shows low diversity index values when measured at the TE superfamily level

Diversity indices are mathematical measures of diversity within a community. In ecology, they are widely used to summarize species diversity within an ecological community, although they are also used in other fields (*e.g.*, economics). Diversity indices take into account species richness (the total number of species present) and evenness (based on the proportional abundance of each species) [46]. Within genome biology, richness can summarize the total number of TE types (*e.g.*, TE superfamilies) and evenness can summarize the proportion of the genome occupied by each TE type [47–50]. We calculated two commonly used diversity indices — the Shannon index and the Gini-Simpson index [51,52] — on the caecilian TE community, as well as the TE communities from ten other vertebrates spanning a range of genome sizes and types of datasets. Genome sizes ranged from 0.4 Gb (the pufferfish *T. rubripes*) to 55 Gb (the hellbender salamander *Cryptobranchus alleganiensis*). Datasets ranged from full genome assemblies to low-coverage genome skims. The Shannon index quantifies the uncertainty in identity of an individual drawn at random from a community. The Gini-Simpson index quantifies the probability that two individuals drawn at random from a community are different types, and it gives more weight to dominant (*i.e.*, most abundant) species. Results are summarized in **Table 3**. The Shannon index ranges from 0.9 (chicken, the least diverse) to 2.41 (green anole lizard, the most diverse). The Gini-Simpson index ranges from 0.5 (chicken, the least diverse) to 1 (pufferfish, the most diverse). By both indices, the caecilian has the second-least diverse genome of the 11 total genomes compared. There is no overall correlation between genome size and TE diversity using either index.

Table 3 Diversity indices summarizing the TE communities from 11 vertebrate genomes

Species	Common name	Genome size (Gb)	Shannon index	Gini-Simpson index	Dataset
Takifugu rubripes	Pufferfish	0.4	2.10	1.00	Full genome assembly
Gallus gallus	Chicken	1.3	0.90	0.50	Full genome assembly
Xenopus tropicalis	Western clawed frog	1.7	2.24	0.90	Full genome assembly
Anolis carolinensis	Green anole lizard	2.2	2.41	0.91	Full genome assembly
Homo sapiens	Human	3.1	1.69	0.79	Full genome assembly
Ichthyophis bannanicus	Banna caecilian	12.2	1.45	0.67	~ 0.1× genome skimming
Desmognathus ochrophaeus	Allegheny Mountain dusky salamander	15	1.61	0.71	~ 0.01× genome skimming
Batrachoseps nigriventris	Black-bellied slender salamander	25	2.18	0.86	~ 0.01× genome skimming
Ambystoma mexicanum	Mexican axolotl salamander	32	2.26	0.89	Full genome assembly
Aneides flavipunctatus	Speckled black salamander	44	1.96	0.78	~ 0.01× genome skimming
Cryptobranchus alleganiensis	Hellbender salamander	55	2.02	0.84	~ 0.01× genome skimming

Most TE superfamilies are active in the *I. bannanicus* genome

For each of the 19 TE superfamilies accounting for ≥ 0.005% of the genome, the overall amplification history was summarized by plotting the genetic distances between individual reads (representing TE loci) and the corresponding ancestral TE sequences as a histogram with bins of 1%. Of these 19 TE superfamilies, 17 of the resulting distributions showed characteristics of ongoing or recent activity (*i.e.*, presence of TE sequences < 1% diverged from the ancestral sequence and a unimodal, right-skewed, J-shaped, or monotonically decreasing distribution) (**Figure 1**). Six of these showed essentially unimodal, right-skewed distributions: LTR/*ERV*, DIRS/*DIRS*, LINE/*Jockey*, LINE/*RTE*, TIR/*piggyBac*, and TIR/*Sola*. Additional three showed essentially unimodal, right-skewed distributions with a spike in sequences < 1% diverged from the ancestral sequence: SINE/*7SL*, TIR/*hAT*, and TIR/*Tc1–Mariner*. A single superfamily — PLE/*Penelope* — showed a left-skewed, J-shaped distribution. These ten distributions suggest TE superfamilies that continue to be active today, but whose accumulation peaked at some point in the past. In contrast, six TE superfamilies showed essentially monotonically decreasing distributions with a maximum at < 1% diverged from the ancestral sequence: LTR/*Gypsy*, DIRS/*Ngaro*, LINE/*L1*, TIR/*CACTA*, TIR/*PIF–Harbinger*, and Maverick/*Maverick*. SINE/*5S* has a bimodal distribution with a maximum

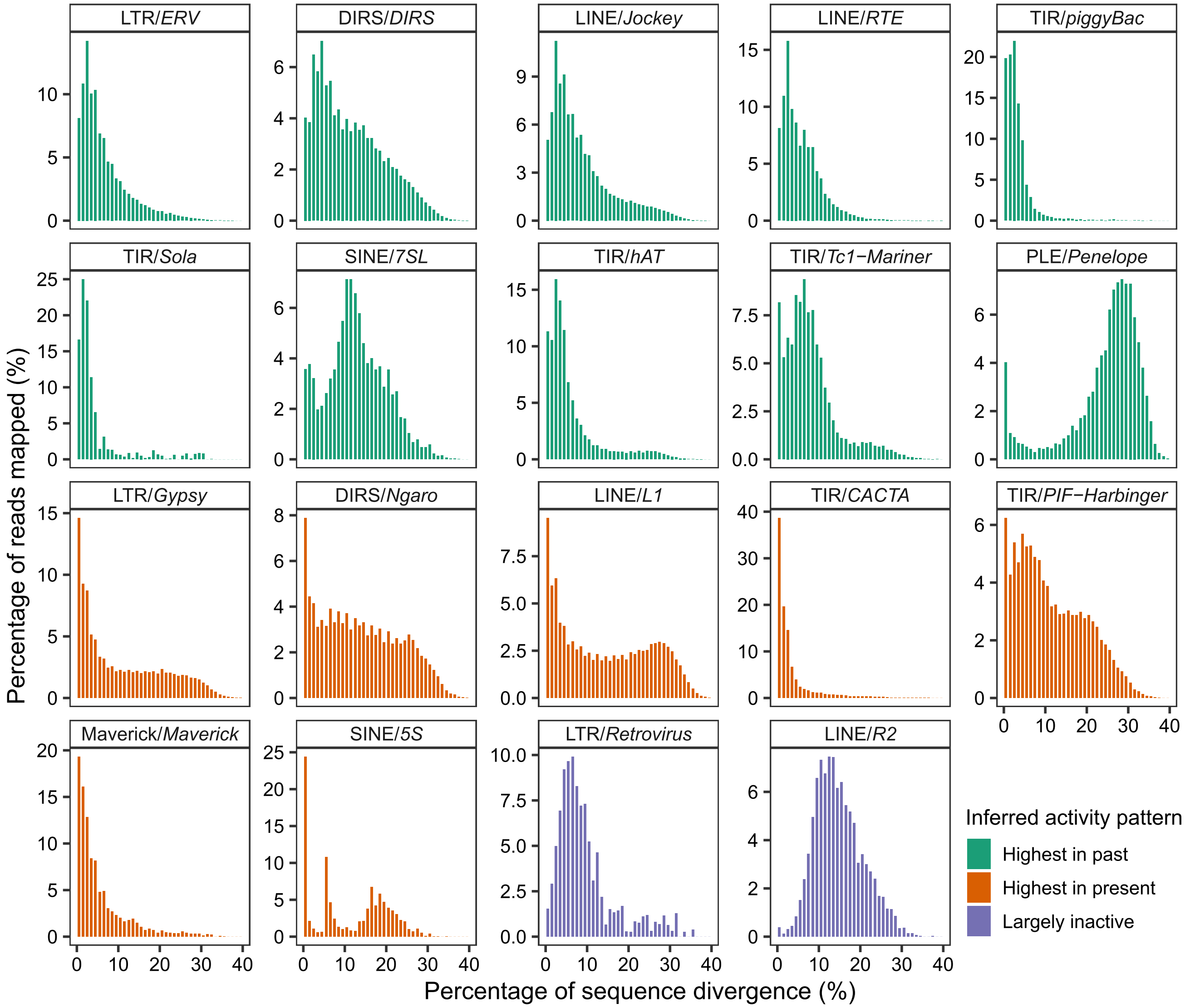

Figure 1 Amplification plots for TE superfamilies

The majority of the amplification plots (17/19) suggest current superfamily activity. Note that the y-axes differ in scale. TE, transposable element.

at < 1% diverged from the ancestral sequence. These seven distributions suggest TE superfamilies that continue to be active today at their highest-ever rates of accumulation. Two superfamilies — LTR/*Retrovirus* and LINE/*R2* — appear largely inactive, showing unimodal distributions with few sequences < 1% diverged from the ancestral. For almost all superfamilies, multiple contigs that were 80% identical in sequence to one another were assembled (range 1–8513), suggesting the presence of many families within each superfamily.

Ectopic recombination-mediated deletion levels are lower in *I. bannanicus* than in vertebrates with smaller genomes

Ectopic recombination, also known as non-allelic homologous recombination, occurs between two DNA regions that are similar in sequence, but do not occupy the same locus. Ectopic recombination among LTR retrotransposon sequences can produce deletions that leave behind solo LTRs, which are single terminal repeat sequences that lack the corresponding internal sequence and matching terminal repeat sequence. Thus, the ratio of LTR sequences to internal retrotransposon sequences can be used to estimate levels of ectopic recombination-mediated deletion. Larger genomes like *I. bannanicus* are predicted to have lower levels of deletion [33].

Two superfamilies were selected for ectopic recombination analysis: DIRS/*DIRS*, which accounts for over a quarter of the caecilian genome, and LTR/*Gypsy*, which is one of the two most abundant LTR superfamilies in the caecilian genome at 1.35%, but which dominates other gigantic amphibian genomes [27]. Mean estimates of the total terminal sequence to internal sequence ratio (TT:I) across the 9 DIRS/*DIRS* contigs range from 1.2:1 to 0.7:1, depending on the minimum alignment length for reads (**Figure 2**). Mean TT:I estimates across the 17 LTR/*Gypsy* contigs range from 1.3:1 to 1.2:1. Values of 1:1 are expected in the absence of ectopic recombination-

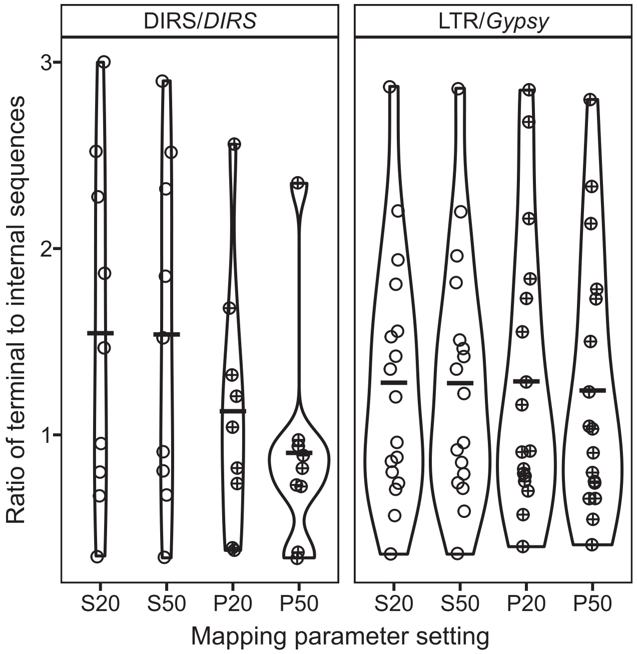

Figure 2 Ratio of total terminal sequence to internal sequence for two TE superfamilies

A ratio of 1:1 is expected in the absence of ectopic recombination-mediated deletion. S, single-end alignment; P, paired-end alignment. 20/50: minimum alignment score (local mode).

mediated deletion. The higher sensitivity of DIRS/*DIRS* than LTR/*Gypsy* to the minimum alignment length parameter value likely reflects the shorter length of the terminal sequence in DIRS/*DIRS* than in LTR/*Gypsy* (150 bp *vs*. 744 bp); the 0.7:1 TT:I value for DIRS/*DIRS* is likely an underestimate. Variation in the TT:I ratio among contigs in each superfamily was similar (Figure 2) and lower than the ranges reported in vertebrates with more typically sized (*i.e*., smaller) genomes [33].

For both superfamilies, ectopic recombination-mediated deletion levels in the caecilian (TT:I ratio ~ 1.2:1) are similar to the low levels estimated from four gigantic salamander genomes (TT:I ratios 0.55:1 to 1.25:1 for *Aneides flavipunctatus*, *Batrachoseps nigriventris*, *Bolitoglossa occidentalis*, and *Bolitoglossa rostrata*) and below the levels estimated from vertebrates with more typically sized (*i.e*., smaller) genomes (TT:I ratios 1.7:1 to 3.35:1 for *Anolis carolinensis*, *Danio rerio*, *Gallus gallus*, *Homo sapiens*, and *Xenopus tropicalis* [33]. TT:I ratios measured for LTR/*Gypsy* in two salamander species (*A. flavipunctatus* and *B. nigriventris*) are 0.9:1 and 1.25:1, respectively, encompassing the value for *I. bannanicus* LTR/*Gypsy*.

If deletion levels were the same between the two superfamilies in the *I. bannanicus* genome, the DIRS/*DIRS* TT:I ratio would be expected to be lower than the LTR/*Gypsy* TT:I ratio because of the structure of DIRS/*DIRS*; it has inverted terminal repeats and internal complementary regions [53,54] that are expected to produce incomplete deletion of the internal sequence following ectopic recombination. The higher TT:I ratio actually estimated in DIRS/*DIRS* may reflect the greater abundance of this superfamily, which increases the number of potential off-targets for recombination, offsetting both the incomplete deletion of the internal sequence and the shorter terminal sequences in DIRS/*DIRS* that would predict lower levels of deletion [55].

Autonomous and non-autonomous TEs are transcribed in *I. bannanicus*

To annotate transcriptome contigs containing autonomous TEs (*i.e*., those with open reading frames encoding the proteins necessary for transposition), BLASTx was used against the Transposable Element Protein Database (RepeatPeps.lib, http://www.repeatmasker.org/). To annotate contigs containing non-autonomous TEs that lack identifiable open reading frames, RepeatMasker was used with our caecilian-derived genomic repeat library of non-autonomous TEs. To identify contigs that contained an endogenous caecilian gene, the Trinotate annotation suite was used [56]. 38,584 contigs were annotated as endogenous (*i.e*., non-TE-derived) caecilian genes. 53,106 contigs were annotated as autonomous TEs using BLASTx against the Transposable Element Protein Database (RepeatPeps.lib). Additional 2658 contigs were annotated as non-autonomous TEs using the caecilian TRIM-, LARD-, SINE- and MITE-annotated genomic contigs. 1445 contigs were annotated as both autonomous TEs and endogenous caecilian genes, and additional 342 were annotated as both non-autonomous TEs and endogenous caecilian genes (**Table 4**).

Of the 20 most highly expressed putative "TE/gene" contigs, ten were confirmed to have annotations for both a

Table 4 Overall summary of transcriptome annotation (contigs with TPM ≥ 0.01)

	No. of contigs (percentage of total contigs)	Summed TPM (percentage of total expression)	Maximum TPM	Minimum TPM	Average TPM	Mean contig length (bp)
Endogenous gene	38,584 (13.3%)	295,759 (29.6%)	10,112.76	0.01	7.7	2086
Autonomous TE	53,106 (18.4%)	131,793 (13.2%)	476.25	0.01	2.5	570
Non-autonomous TE	2658 (0.9%)	8484 (0.9%)	371.09	0.01	3.2	785
Gene/autonomous TE	1445 (0.5%)	4859 (0.5%)	383.94	0.01	3.7	2161
Gene/non-autonomous TE	342 (0.1%)	1584 (0.2%)	198.8	0.01	4.6	2800
Unannotated	193,245 (66.8%)	555,776 (55.6%)	8224.66	0.01	2.9	537
Total	289,380 (100%)	1,000,006 (100%)	10,112.76	0.01	3.5	763

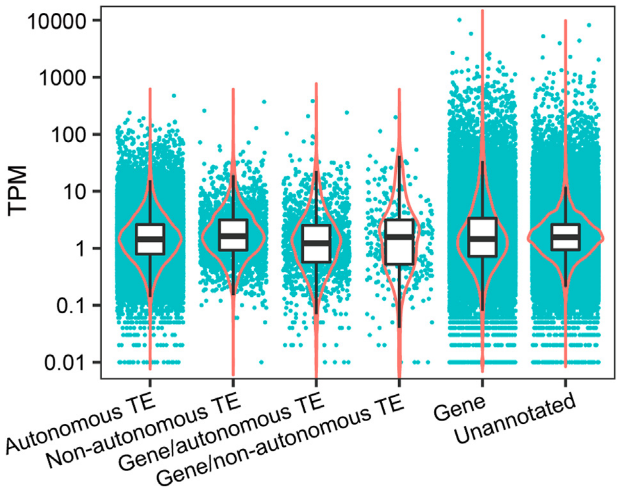

Figure 3 Expression levels of genes and TEs

Black lines and white boxes show median and interquartile range values. Red lines show probability densities. TPM, transcripts per million.

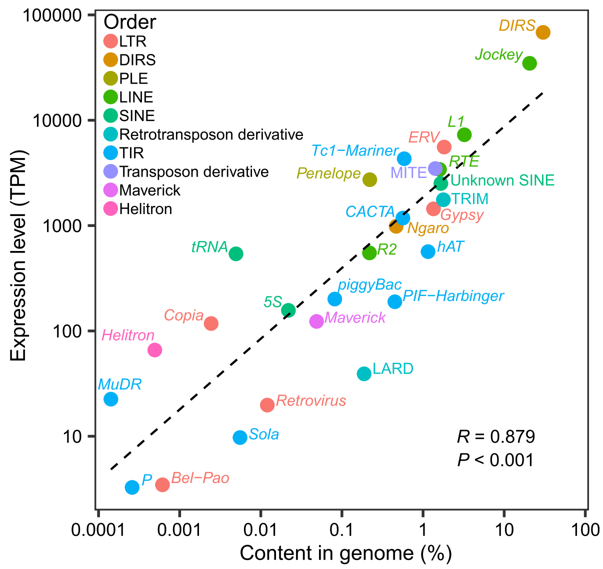

Figure 4 Genomic abundance and somatic expression level of TE superfamilies are strongly correlated

TE and a gene with non-overlapping ORFs. Of these, the TE was upstream of the gene in eight cases and downstream in two cases. Six of the upstream TEs were autonomous and thus contained ORFs; four of these were encoded on the same strand as the gene (two in-frame, two not in-frame) and two were encoded on the opposite strand. One of the two downstream TEs was autonomous, and it was encoded on the opposite strand from the gene. Although requiring further validation, these results suggest that at least some TE/gene pairs are co-transcribed, a way in which TE insertions can regulate gene expression [57]. One contig had overlapping annotations of a gene and a TE, a pattern that could reflect either convergence in sequence or exaptation of a TE [58].

Expression of TEs correlates with their genomic abundance in *I. bannanicus*

Among the transcriptome contigs with transcripts per million (TPM) $\geq$ 0.01, autonomous TEs account for 18.4% of the total transcriptome contigs and 13.2% of the overall somatic transcriptome (summed TPM = 131,793) (**Figure 3**; Table 4). Non-autonomous TEs account for 0.9% of the total transcriptome contigs and 0.9% of the somatic transcriptome (summed TPM = 8484). Contigs annotated both as TEs and endogenous caecilian genes account for 0.6% of the total annotated transcriptome contigs and 0.7% of the somatic transcriptome (summed TPM = 6443). Endogenous (non-TE-derived) caecilian genes account for 13.3% of the total transcriptome contigs and 29.6% of the somatic transcriptome (summed TPM = 295,759). Unannotated contigs account for 66.8% of the total transcriptome contigs and 55.6% of the somatic transcriptome (summed TPM = 555,776). Five superfamilies (*I*, *Zisupton*, *Kolobok*, *Academ*, and *Crypton*) were detected at low expression levels in the transcriptome, but were not initially detected in the genomic data; mapping the genomic reads to these transcriptome contigs with Bowtie2 identified $\leq$ 3 reads per superfamily, indicating their extremely low frequency in the genome. In contrast, only one superfamily (SINE/*7SL*) was detected in the genomic data but not the transcriptome data.

Class I TEs (retrotransposons) are over ten times more abundant in the transcriptome than Class II TEs (summed TPM = 130,076 and 10,202, respectively). Within the retrotransposons, the DIRS/*DIRS* superfamily is the most highly expressed, followed by LINE/*Jockey* and LINE/*L1*; these three superfamilies are also the most abundant in the genome. For almost all retrotransposon superfamilies, hundreds to thousands of transcriptome contigs that were 80% identical in sequence to one another were assembled (range 1–12,652), suggesting the simultaneous activity of many families within all of the superfamilies in the caecilian somatic transcriptome. Large differences (up to ~ 10,000-fold) in expression were detected among the different contigs within superfamilies, suggesting variable expression levels across loci and among families; we interpret this pattern with caution because of the challenges of uniquely mapping short reads to contigs of similar sequence. Within the DNA transposons, TIR/*Tc1–Mariner*, TIR/*CACTA*, and TIR/*hAT* are the most highly expressed superfamilies, and MITEs (transposon derivatives) are expressed at similar levels to these superfamilies, although they lack their own promoters. These four types of sequences are also the four most abundant types of DNA transposons in the genome, although their genomic abundance is not perfectly correlated with their relative expression levels. For the DNA transposons, tens to hundreds of contigs that were 80% identical in sequence to one another were assembled (range 2–421), and up to ~ 1000-fold differences in expression were detected among contigs. Overall, a strong correlation was detected between genomic abundance of a TE superfamily and its overall somatic expression level (R = 0.879, P < 0.001) (**Figure 4**). Although germline expression data are required to analyze the relationship between TE transcription and TE-activity-driven genome evolution, the somatic data nevertheless provide valuable information on the cellular resources allocated to transcription of a greatly expanded TE community.

Discussion

Repeat element landscape characterization in large genomes

Large, repetitive genomes have proven difficult to assemble and annotate with the computational power and analytical tools applied to archaeal, bacterial, and smaller eukaryotic genomes [59,60]. Recent successful genome sequencing efforts aimed at the 32 Gb genome of *Ambystoma mexicanum*, a laboratory model salamander species, leveraged multiple types of data (*i.e.*, optical mapping, short- and long-read genomic sequence data, transcriptomic data, linkage mapping, and fluorescence *in situ* hybridization) and a new assembler designed to minimize compute time and storage requirements [30,61]. These projects yielded fundamental insights into the structure and evolution of vertebrate chromosomes. They also advanced understanding of the transposons that make up large genomes, adding to research on the 20-Gb Norway spruce and the 22-Gb loblolly pine and 31-Gb sugar pine [62–64]. This depth of analysis, however, remains infeasible for non-model organisms with large genomes, whose study is nevertheless required to understand how TEs drive genome biology. Our work affirms the power of low-coverage sequence data to reveal the overall repeat element landscape of large genomes, an approach applied most often in plants (which include the majority of huge genomes) [65,66]. We argue that this overall landscape, although it lacks the positional information about individual TE insertions that genome assemblies provide, contains much information that can reveal the evolutionary processes that drive assembly and stability of TE communities.

Repeat element landscapes are informative because they include data on the abundance, diversity, and activity of TEs that make up the overall TE community in a genome. Models of TE dynamics predict different values for TE abundance, diversity, and activity depending on levels of purifying selection, silencing, and deletion of TEs. Despite much progress, these forces remain challenging to measure directly. Thus, repeat element landscapes provide a more feasible approach to validating these models and advancing our understanding of TE dynamics in natural systems.

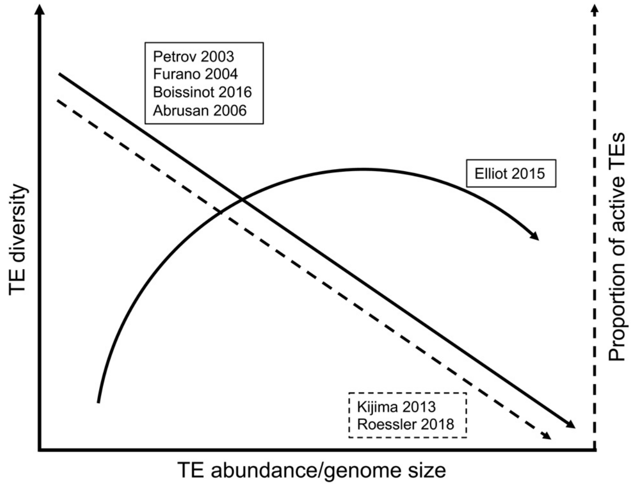

Figure 5 Predicted relationships between TE abundance (genome size), TE diversity, and proportion of active TEs from seven different models

Repeat element landscapes from large genomes provide tests of models of TE dynamics

Large genomes are especially powerful data points because they represent extreme values of TE abundance, and models of TE dynamics make specific predictions about the effects of TE abundance on TE diversity and activity. We first summarize and highlight the differences among several of these models here (**Figure 5**):

Petrov 2003 — TE deletion is caused by ectopic recombination between similar TE sequences. Rates of ectopic recombination/deletion are typically higher in smaller genomes and lower in larger genomes. Thus, smaller genomes are predicted to select for more diverse TE communities, and larger genomes should allow less diverse TE communities [55,67]. This model predicts an inverse relationship between genome size and TE diversity.

Furano 2004 — Because ectopic recombination can cause harmful deletions, it is one of the primary reasons for TEs' deleterious effects on host fitness. Thus, genomes with lower ectopic recombination/deletion rates are more permissive to TE activity, allowing the accumulation of more TEs (increased genome size) as well as increased TE activity and out-competition of many TE lineages by the lineage that most successfully exploits host replication factors [68]. Like Petrov 2003, this model predicts an inverse relationship between genome size and TE diversity, but for different reasons.

Boissinot 2016 — Genomes with lower ectopic recombination/deletion rates have higher levels of insertion of active TE copies into the genome. In addition to yielding a larger genome, this higher number of active TE copies triggers an arms race to control transposition, and the arms race leads to a decrease in diversity (*i.e.*, only one family active at a time) [69]. Like Petrov 2003 and Furano 2004, this model also predicts an inverse relationship between genome size and TE diversity, but for still different reasons.

Abrusan 2006 — TE diversity and activity levels were modeled with a system of differential equations that includes parameters for the number of TE strains, the number of active TE insertions, TE replication rates, the strength of specific silencing of TEs (representing small-RNA-mediated silencing), cross-reactivity of silencing, and TE inactivation by mutation or selection [70]. Although their model did not specifically address genome size, it did predict that increased genome size would be associated with decreased TE diversity if 1) larger genomes harbor more active TE copies and 2) cross-reactive silencing exists among TEs. Under these conditions, competition among the TEs to evade cross-reactive silencing would lead to decreased TE diversity. Cross-reactive silencing in this model is not sequence-specific; this is relevant because silencing of TEs by small-RNA-mediated silencing (*e.g.*, the piRNA pathway) is sequence-specific, but can have some off-target effects. These off-target effects are predicted to have the opposite effect on TE diversity than non-sequence-specific cross-reactive silencing; they should select for higher TE diversity. Overall, the predictions for genome size and TE diversity from this model are complex, depending on the relative strengths of specific TE silencing, off-target specific TE silencing, and cross-reactive (*i.e.*, sequence-independent) silencing.

Elliot 2015 — Based on empirical comparisons across genomes of different sizes, TE diversity was proposed to increase with TE abundance until genomes reach moderate size, but extremely large genome sizes were proposed to reflect the proliferation of only a subset of TE diversity by unspecified mechanisms [71]. This predicts an inverse relationship between genome size and TE diversity at the largest genome sizes.

Kijima 2013 — TE evolution was modeled using a population genetic simulation framework that includes parameters for transposition, TE deletion, purifying selection on TE copy number (genome size), and degeneration into inactive copies [72]. When copy number selection is strong (*i.e.*, genome size remains small), the total number of TEs is lower, but the proportion of active copies of TEs is higher. When copy number selection is weak (*i.e.*, genome size is allowed to increase), the total number of TEs is higher, but the proportion of active copies of TEs is lower. This reflects competition among TEs to occupy limited available spaces in the genome. This model does not consider TE diversity — it models only a single TE strain — but it predicts an inverse relationship between genome size and proportion of the total TE community that is actively transposing. Interestingly, they find that excision (deletion) rate is not a predictor of copy number.

Roessler 2018 — TE evolution was modeled using ordinary differential equations including parameters for TE transposition, RNA-mediated TE silencing, TE deletion, and TE copy number (genome size) [73]. This model predicts that, under low rates of TE deletion, TE copy number and genome size increase, and the proportion of active TEs goes down because the host organism can use the accumulating TE sequences as templates for producing more small silencing RNAs and, thus, inactivate a higher proportion of TE sequences. Like Kijima 2013, this model predicts an inverse relationship between genome size and proportion of the total TE community that is actively transposing, but for different (albeit complementary) reasons.

Does the TE landscape of the large caecilian genome — with its high levels of TE abundance and low levels of TE ectopic recombination/deletion — fit the predictions of these models or allow discrimination among them? Most share a prediction of decreased TE diversity in large genomes. Measured at the coarse-grained level of number of superfamilies present (*i.e.*, taking into account richness only) [71], *I. bannanicus* does not fit this prediction; at least 25 TE superfamilies are present in the genome (as detected by our genomic and transcriptomic analyses). However, genome expansion in *I. bannanicus* is correlated with high DIRS/*DIRS* and LINE/*Jockey* superfamily abundance, consistent with Elliot 2015′s prediction that gigantic genomes would reflect proliferation of a limited subset of all TEs. This expansion decreases evenness, despite the maintenance of high richness; this is exactly the type of change in overall diversity that is captured by the indices we advocate here.

Comparing the diversity indices calculated for *I. bannanicus* with the ten other vertebrate genomes (Table 3) allows a direct test of the relationship between genome size (*i.e.*, TE abundance) and TE diversity. Because the genomes included were analyzed with different sequencing depths, we favor the Gini-Simpson index as it is less affected by rare species (TE superfamilies), which are more likely missed in the low-coverage datasets (*e.g.*, *I*, *Zisupton*, *Kolobok*, *Academ*, and *Crypton*; Table 2). Consistent with model predictions, the smallest genome (*T. rubripes*) has the highest TE diversity, and the three most diverse genomes (*T. rubripes*, *A. carolinensis*, and *X. tropicalis*) are three of the four smallest (Table 3). However, among the large amphibian genomes — *I. bannanicus* and the five salamanders — there is no relationship between TE abundance and diversity. Furthermore, the chicken genome is the least diverse, and it is the second-smallest.

However, the lack of relationship between TE abundance and diversity, measured here at the TE superfamily level for 11 species, does not necessarily refute the models of TE dynamics that predict decreased TE diversity with increased TE abundance. Diversity exists within TE superfamilies as well; TE families are typically operationally defined based on Wicker's 80/80/80 rule, and subfamilies can be further split based on pairs of substitutions overrepresented in TE alignments that are unlikely to have arisen independently by chance [7,74]. It is not yet clear what levels of sequence divergence translate into functionally relevant "TE diversity" in the models summarized above. More specifically, TE diversity implies: 1) TE sequences that have diverged beyond the ability to ectopically recombine in Petrov 2003, 2) TE sequences that have diverged enough to differ in ability to monopolize host replicative resources in Furano 2004, 3) TE sequences that have diverged enough to (sequentially) out-evolve host silencing machinery in Boissinot 2016, and 4) TE sequences that have diverged enough to differ in their silencing by cross-reactive (*i.e.*, non-sequence-specific) or off-target (*i.e.*, sequence-specific, but tolerant of mismatches) TE silencing mechanisms in Abrusan 2006. We still lack sufficient information about TE silencing to define the levels of sequence divergence likely to accompany these changes in TE dynamics. Thus, it is not yet clear whether diversity indices are best focused at the TE superfamily, family, or subfamily levels. As an example, the chicken genome is the least diverse measured here at the level of TE superfamilies because CR1 elements dominate the genome; however, diversity exists within the CR1 elements that may be functionally relevant [75]. To move the field forward, we advocate using Shannon and Simpson indices at the levels of TE family and subfamily (in addition to superfamily) when datasets allow. When this is impossible — for example, when working with low-coverage shotgun data from gigantic genomes like *I. bannanicus* — we advocate calculating diversity indices at the superfamily level, but also reporting the numbers of genomic and transcriptomic contigs at the level of 80% sequence identity as a tractable within-superfamily approximation of TE diversity (Table 2). This measure is analogous to species richness and lacks information on evenness (because of the challenges of uniquely mapping short reads to contigs of similar sequence), so it is less informative than diversity indices. However, the reporting of this measure by researchers studying diverse organisms would allow progress towards rigorously testing the relationship between genome size and TE diversity. Furthermore, it may identify specific taxa as appropriate models to examine evolutionary changes in TE silencing pathways. For example, *I. bannanicus* has a large genome but appears to maintain a high number of TE families (Table 2), suggesting that its TE silencing machinery includes high levels of off-target silencing [70].

In addition to predicting low TE diversity, models of TE dynamics predict a decreased proportion of active TEs as TE abundance and genome size increase. Of the 19 caecilian TE superfamilies for which amplification histories were examined, 17 appear to have ongoing activity (Figure 1). These results are largely corroborated by the (albeit somatic) expression data, although SINE/*7SL* and LINE/*R2* show conflicting patterns in the genomic and transcriptomic data (Figure 1; Table 2). TE expression is necessary, but insufficient, for TE activity, but it is a tractable proxy for TE activity. Taken together, these datasets suggest near-complete activity at the TE superfamily level in the *I. bannanicus* genome. At the levels of TE family or individual insertions, activity is difficult to assess with our data; however, the presence of multiple transcriptome contigs at the level of 80% sequence identity within superfamilies minimally suggests the expression of multiple families. Our recommendation that researchers report the number of transcriptomic TE contigs at the level of 80% sequence identity will also allow progress towards rigorously testing the relationship between genome size and TE activity, as will adoption of recent methods to measure locus-specific expression when datasets allow [76].

Overall, ~ 15% of all somatic tissue transcripts of *I. bannanicus* are TEs (Table 4). Comparing overall levels of TE expression across different genome sizes remains difficult because TE expression in general is understudied [76], transcriptome size differences that accompany genome size differences are typically not quantified [77], and TE annotation and expression quantification methods vary across studies [38,78–80]. As another step towards testing the relationship between genome size and TE activity, we advocate annotation of both autonomous and non-autonomous TE transcripts and reporting of expression levels of TEs and endogenous genes (Figure 3; Tables 2 and 4).

Taken together, our work lays a foundation for comparative genomic analyses that link properties of TE communities — abundance, diversity, and activity — to genome size evolution. Such analyses, in turn, will reveal whether the divergent TE assemblages found across convergent examples of genomic gigantism reflect more fundamental shared features of TE/host genome evolutionary dynamics.

Materials and methods

Specimen information

We collected a single male adult caecilian (*I. bannanicus*) from the species' type locality (E′101.3887, N′21.8724) in Mengxing County, Yunnan province, China. The individual had a total body length of 16.0 cm and a body mass of 4.8 g. Following dissection, the carcass was fixed in formalin and transferred to 70% ethanol.

Genome size estimation

Blood smears were prepared from the formalin-fixed *I. bannanicus* specimen as well as a formalin-fixed salamander (*Plethodon cinereus*) with an appropriate genome size to serve as the reference standard (22.14 Gb) [25]. Blood cells were pipetted onto glass microscope slides and air-dried, then hydrated for 3 min in distilled water. Slides were 1) hydrolyzed in 5 N HCl for 20 min at 20 °C and washed three times in distilled water for 1 min each, 2) stained with Schiff's reagent in a Coplin jar for 90 min at 20 °C, 3) soaked in three changes of 0.5% sodium metabisulfite solution for 5 min each and rinsed in three changes of distilled water for 1 min each, and 4) dehydrated in 70%, 95%, and 100% ethanol for 1 min each, air-dried, and mounted in immersion oil and cover glass.

The stained slides were photographed using an Olympus BX51 compound microscope fitted with a Spot Insight 4 digital camera for image analysis. Stained nuclei were photographed under 100× oil immersion and the integrated optical densities were measured using ImagePro software. Genome size for *I. bannanicus* was calculated by comparing the mean optical density to that of the reference standard, *P. cinereus*.

Genomic shotgun library creation, sequencing, and assembly

Total DNA was extracted from muscle tissue using the modified low-salt CTAB extraction of high-quality DNA procedure [81]. DNA quality and concentration were assessed using agarose gel electrophoresis, a NanoDrop Spectrophotometer (ThermoFisher Scientific, Waltham, MA), and a Qubit 2.0 Fluorometer (ThermoFisher Scientific). A PCR-free library was prepared using NEBNext Ultra DNA Library Prep Kit for Illumina. Sequencing was performed on two lanes of a Hiseq2500 platform (PE250). Library preparation and sequencing were performed by the Beijing Novogene Bioinformatics Technology Co. Ltd. Raw reads were quality-filtered and trimmed of adaptors using Trimmomatic-0.36 [82] with default parameters. In total, the genomic shotgun dataset included 7,785,846 reads. After filtering and trimming, 7,275,133 reads covering a total length of 1,635,569,256 bp remained. Thus, the sequencing coverage is 0.134. Filtered, trimmed reads were assembled into contigs using dipSPAdes 3.11.1 [83] with default parameters, yielding 130,417 contigs with an N50 of 740 bp and a total length of 1,560,938,851 bp.

Mining and classification of repeat elements

The PiRATE pipeline was used as in the original publication [44], including the following steps: 1) Contigs representing repetitive sequences were identified from the assembly using similarity-based, structure-based, and repetitiveness-based approaches applied non-sequentially. The similarity-based detection programs included RepeatMasker [84] and TE-HMMER [85]. The structure-based detection programs included MITE-Hunter [86], SINE-Finder [87], HelSearch [88], LTRharvest [89], and MGEScan-non-LTR [90]. The repetitiveness-based detection programs included TEdenovo [91] and RepeatScout [92]. 2) Contigs representing repeat family consensus sequences were also identified from the cleaned, filtered, unassembled reads with dnaPipeTE [93], which uses Trinity on subsamples of single-end reads to produce sets of related repeat consensus sequences (*e.g.*, representing multiple subfamilies within a TE family). 3) Contigs identified by each individual program in Steps 1 and 2, above, were filtered to remove those < 100 bp in length and clustered with

CD-HIT-est [94] to reduce redundancy (100% sequence identity cutoff). This yielded a total of 62,699 contigs. 4) All 62,699 contigs were then clustered together with CD-HIT-est (100% sequence identity cutoff), retaining the longest contig and recording the program that classified it. 1860 contigs were filtered out at this step, and the majority (1669) were contigs identified by RepeatMasker and TE-HMMER that were identical in sequence but differed in length. 5) Repeat contigs were annotated as TEs to the levels of order and superfamily in Wicker's hierarchical classification system [7], modified to include several recently discovered TE superfamilies using PASTEC [45], and were checked manually to filter chimeric contigs and those annotated with conflicting evidence. 6) All classified repeats ("known TEs" hereafter), along with the unclassified repeats ("unknown repeats" hereafter) and putative multi-copy host genes, were combined to produce a caecilian-derived repeat library.

Characterization of the overall repeat element landscape

Overlapping paired-end reads were merged using PEAR v.0.9.11 [95] with the following parameter values based on our library insert size and trimming parameters: min-assemble-length 36, max-assemble-length 490, min-overlap size 10. After merging the remaining paired-end reads, 6,628,808 shotgun reads remained, with an average and a total length of 236 and 1,560,938,851 bp, respectively. To calculate the percentage of the caecilian genome composed of different TEs, the shotgun reads (including both merged reads and singletons) were masked with RepeatMasker v-4.0.7 using two versions of our caecilian-derived repeat library: one that included the unknown repeats and one that excluded them. In both cases, simple repeats were identified using the Tandem Repeat Finder module implemented in RepeatMasker. The overall results were summarized at the levels of TE class, order, and superfamily. For each superfamily, we then collapsed the contigs to 95% and 80% sequence identity using CD-HIT-est to provide an overall view of within-superfamily diversity; 80% is the sequence identity threshold used to define TE families [7].

TE community diversity

Diversity of the overall TE community in *I. bannanicus* was summarized using the Shannon index $H' = -\sum P_i \ln(P_i)$ and the Simpson index $D_1 = 1 - \sum P_i^2$ (*i.e.*, the Gini-Simpson index), where P_i is the proportion of sequences belonging to TE superfamily i [51,52]. In analogous applications of these diversity indices to ecological communities, P_i is the proportion of individuals that belong to species i. To provide context for the *I. bannanicus* results, Shannon and Simpson indices were also calculated for other vertebrate genomes representing diversity in genome size as well as type of dataset. *T. rubripes* (pufferfish, 0.4 Gb), *G. gallus* (chicken, 1.3 Gb), *X. tropicalis* (Western clawed frog, 1.7 Gb), *A. carolinensis* (green anole lizard, 2.2 Gb), and *H. sapiens* (human, 3.1 Gb) all have full genome assemblies. For these five species, the perl script parseRM.pl [96] was used to parse the raw output files downloaded from www.repeatmasker.org and obtain the percentage of the genome occupied by each identified superfamily; ambiguous classifications (*i.e.*, to the level of order or class) were excluded. *A. mexicanum* (Mexican axolotl, a model salamander, 32 Gb), which has a much larger genome and, consequently, less complete genome assembly, was also included; percentages of the genome occupied by each identified superfamily were obtained from a previous study [30]. Finally, four other salamanders that encompass a range of genome sizes were included, each represented by low-coverage genome-skimming shotgun data: *Desmognathus ochrophaeus* (15 Gb), *B. nigriventris* (25 Gb), *A. flavipunctatus* (44 Gb), and *C. alleganiensis* (55 Gb). Percentages of each genome occupied by identified superfamilies were obtained from a previous study [32].

Amplification history of TE superfamilies

To summarize the overall amplification history of TE superfamilies and test for ongoing activity, the perl script parseRM.pl [96] was used to parse the raw output files from RepeatMasker (.align) and report the sequence divergence between each read and its respective consensus sequence (parameter values = –l 50,1 and –a 5). The repeat library used to mask the reads comprised the 50,471 TE contigs classified by the PiRATE pipeline and clustered at 100% sequence identity. Each TE superfamily is therefore represented by multiple consensus contigs that represent ancestral sequences likely corresponding to the family and subfamily TE taxonomic levels (*i.e.*, not the distant common ancestor of the entire superfamily). For each superfamily, histograms were plotted to summarize the percent divergence of all reads from their closest (*i.e.*, least divergent) consensus sequence. These histograms do not allow the delineation between different amplification dynamics scenarios (*i.e.*, a single family with continuous activity *versus* multiple families with successive bursts of activity). Rather, these global overviews were examined for overall shapes consistent with ongoing activity (*i.e.*, the presence of TE loci < 1% diverged from the ancestral sequence and a unimodal, right-skewed, J-shaped, or monotonically decreasing distribution).

Ectopic recombination-mediated deletion of LTR/*Gypsy* and DIRS/*DIRS* elements

All genomic contigs > 3000 bp in length that were annotated to LTR/*Gypsy* were *de novo* annotated using LTRpred to identify terminal and internal sequences [97]. Internal and terminal sequences were further confirmed by manually checking for internal TE domains using NCBI BLASTx (https://blast.ncbi.nlm.nih.gov/Blast.cgi?PROGRAM=blastx&PAGE_TYPE=BlastSearch&LINK_LOC=blasthome) and for terminal repeat sequences using the NCBI-Blast2suite to align each contig sequence against itself. DIRS/*DIRS* superfamily elements have a different structure than LTR retrotransposons; their terminal repeats are inverted. However, because they also include internal sequences complementary to the terminals that facilitate rolling-circle amplification [53,54], their structure includes direct repeats that are expected to undergo ectopic recombination to eliminate much of the internal sequence and one copy of the direct repeat sequence, although to our knowledge this has not been previously investigated. Although these deletions would not produce canonical solo

LTRs, they, too, would produce elevated abundances of terminal sequences relative to internal sequences. Typical DIRS/*DIRS* structure was confirmed visually and by using the NCBI-Blast2suite to align each contig sequence against itself, and contigs that lacked the complete structure were removed from further analysis. Internal sequences for both superfamilies were conservatively defined to be bounded by the first and last TE domains. This yielded a total of 9 DIRS/*DIRS* contigs and 17 LTR/*Gypsy* contigs. DIRS/*DIRS* contigs had an average terminal sequence length of 150 bp (range 61–343 bp) and an average internal sequence length of 5586 bp (range 4810–6012 bp). LTR/*Gypsy* contigs had an average terminal sequence length of 744 bp (range 127–3267 bp) and an average internal sequence length of 1976 (range 243–4306 bp). To estimate levels of terminal sequences (LTRs or TIRs) relative to internal sequences, genomic shotgun reads were mapped to the whole genome assembly using bowtie2 in local alignment mode with very-sensitive-local preset options and otherwise default parameters, increasing the G-value from the default of 20 to 30, 40, and 50 to increase minimum alignment length for reads [98]. This analysis was performed twice: once treating all reads as unpaired and once using merged paired-end reads plus unmerged reads. Average read depths across the terminal and internal portion in each of the 26 focal DIRS/*DIRS* and LTR/*Gypsy* contigs were estimated by scaling the number of hits by the lengths of the terminal and internal regions. From these estimates, the total terminal-to-internal sequence ratio (TT:I) was calculated for each contig. In the absence of ectopic recombination mediated by terminal repeats, this ratio would be 1:1; increasing levels of ectopic recombination would produce ratios > 1:1. We compared the results obtained for the caecilian with similar analyses that included gigantic salamander genomes as well as vertebrates with more typical (*i.e.*, smaller) genomes [33].

Transcriptome library creation, sequencing, assembly, and TE annotation

Total RNA was extracted separately from heart, brain, liver, and tail tissues using TRIzol (Invitrogen). For each sample, RNA quality and concentration were assessed using agarose gel electrophoresis, a NanoPhotometer spectrophotometer (Implen, CA), a Qubit 2.0 Fluorometer (ThermoFisher Scientific), and an Agilent BioAnalyzer 2100 system (Agilent Technologies, CA) requiring an RNA integrity number (RIN) of eight or higher. Equal quantities of RNA from these four tissues were pooled to build a single transcriptome library. Sequencing libraries were generated using the NEBNext Ultra RNA Library Prep Kit for Illumina following the manufacturer's protocol. After cluster generation of the index-coded samples, the library was sequenced on one lane of an Illumina Hiseq 4000 platform (PE 150). Library preparation and sequencing were performed by the Beijing Novogene Bioinformatics Technology Co. Ltd, China. Transcriptome sequences were filtered using Trimmomatic-0.36 with default parameters [82]. Remaining reads were assembled using Trinity 2.5.1 [99]. In total, 34,980,300 transcriptome reads were obtained, with a total length of 5,247,045,000 bp. After filtering, 34,417,105 reads remained, with a total length of 5,027,542,505 bp. The assembly produced 348,822 contigs (*i.e.*, putative assembled transcripts) with the min, N50, max, and total length of contigs equal to 201, 357, 32,175, and 249,943,402 bp, respectively. Of these, 289,380 had expression levels of TPM ≥ 0.01 and were analyzed further.

To annotate transcriptome contigs containing autonomous TEs, BLASTx was used against the Transposable Element Protein Database (RepeatPeps.lib, downloaded from https://github.com/rmhubley/RepeatMasker/blob/master/Libraries/ on April 20, 2019) with an E-value cutoff of 1E–10. To annotate contigs containing non-autonomous TEs, RepeatMasker was used with our caecilian-derived genomic repeat library of non-autonomous TEs (LARD-, TRIM-, MITE-, and SINE-annotated contigs; Table 2) and the requirement that the transcriptome/genome contig overlap was > 80 bp long, > 80% identical in sequence, and covered > 80% of the length of the genomic contig. Contigs annotated as conflicting autonomous and non-autonomous TEs were filtered out. To yield a rough estimate of the number of active TE families per superfamily, CD-HIT-est was used to cluster the contigs annotated to each superfamily at the level of 80% sequence identity.

To identify contigs that contained an endogenous caecilian gene, the Trinotate annotation suite was used with E-value cutoffs of 1E−10 and 1E−5 for BLASTx and BLASTp against the SwissProt database, respectively, and 1E−5 for HMMER against the Pfam database [56]. To identify contigs that contained both a TE and an endogenous caecilian gene (*i.e.*, putative cases where a TE and a gene were co-transcribed on a single transcript), all contigs that were annotated both by RepeatPeps and Trinotate were examined, and the ones annotated by Trinotate to contain a TE-encoded protein (*i.e.*, the contigs where RepeatPeps and Trinotate annotations were in agreement) were not further considered. The remaining contigs annotated by Trinotate to contain a non-TE gene (*i.e.*, an endogenous caecilian gene) and also annotated either by RepeatPeps to include a TE-encoded protein or by RepeatMasker to include a non-autonomous TE were identified for further examination and expression-based analysis.

TE expression

To generate a point estimate of overall TE expression in the somatic transcriptome, transcript abundance levels were quantified with RSEM (because of its capacity to model multi-mapping reads) using the Bowtie short-read aligner. Transcriptome contigs with TPM < 0.01 were filtered out. To yield TE-superfamily-wide expression level estimates, TPM values were summed across all contigs annotated to the same TE superfamily. For comparison, TPM values were summed for all endogenous (*i.e.*, non-TE) caecilian genes. Pearson's correlation coefficient was used to test for a relationship between genomic TE abundance (measured as log-transformed percentage of the genome occupied per TE superfamily) and TE expression level (measured as log-transformed total TPM per TE superfamily). We note that with only a single sample, any more detailed analyses of expression levels are not appropriate. Contigs annotated to contain both TEs and endogenous caecilian genes were excluded from these analyses. Instead, these putative TE/gene contigs were ranked by expression level, and the 20 most highly expressed were examined by eye to determine the spatial relationship between the TE and gene via the BLAST results producing the annotations. Nine contigs with apparently spurious TE annotations (seven of which reflected a single likely mis-annotation of an LTR/Pao protein in the RepeatPeps database) were reclassified as endogenous genes, and the remaining contigs were characterized as having the TE 1) on the same or different strand as the gene, and 2) upstream or downstream of the gene. Finally, TPM values were summed across all putative TE/gene contigs to yield a global estimate of expression levels of TE/gene combinations that are co-transcribed on a single transcript.

Ethical statement

The study specimen was collected and dissected following Animal Care & Use Protocols approved by Chengdu Institute of Biology, Chinese Academy of Sciences.

Data availability

Genomic shotgun and transcriptome sequences have been deposited in the Genome Sequence Archive [100] at the National Genomics Data Center, Beijing Institute of Genomics, Chinese Academy of Sciences / China National Center for Bioinformation (GSA: CRA002184), and are publicly accessible at http://bigd.big.ac.cn/gsa.

CRediT author statement

Jie Wang: Conceptualization, Methodology, Software, Formal analysis, Investigation, Resources, Data curation, Writing - original draft, Writing - review & editing, Visualization, Funding acquisition. **Michael W. Itgen:** Methodology, Software, Formal analysis, Investigation. **Huiju Wang:** Methodology, Software. **Yuzhou Gong:** Resources. **Jianping Jiang:** Methodology. **Jiatang Li:** Methodology. **Cheng Sun:** Methodology, Writing - review & editing. **Stanley K. Sessions:** Investigation, Resources. **Rachel Lockridge Mueller:** Conceptualization, Formal analysis, Investigation, Resources, Writing - original draft, Writing - review & editing, Supervision, Project administration, Funding acquisition. All authors read and approved the final manuscript.

Competing interests

The authors have declared no competing interests.

Acknowledgments

This work was supported by the National Natural Science Foundation of China (Grant No. 31570391 to WJ), the National Key R & D Program of China (Grant No. 2016YFC0503200), and the National Science Foundation of USA (Grant No. 1911585 to RLM). We gratefully acknowledge Xungang Wang, Liming Chang, Lusha Liu, Yiwei Zeng, and Shan Xiong for target tissue dissection; Daniel B. Sloan, Yufeng Wang, Zhiqiang Wu, Evan Forsythe, Aurélie Kapusta, Amanda R. Goldberg, Chaochao Yan, Jiongyu Liu, and Ava Lambert for their expertise in facilitating data analysis; Jérémy Berthelier for help running PiRATE; and Arnaud Le Rouzic and two anonymous reviewers for insightful suggestions for improving the manuscript.

ORCID

0000-0003-4318-8923 (Jie Wang)
0000-0001-9481-0693 (Michael W. Itgen)
0000-0003-0960-8939 (Huiju Wang)
0000-0002-2380-180X (Yuzhou Gong)
0000-0002-1051-7797 (Jianping Jiang)
0000-0003-1799-194X (Jiatang Li)
0000-0001-7476-9224 (Cheng Sun)
0000-0002-9444-028X (Stanley K. Sessions)
0000-0003-3875-1988 (Rachel Lockridge Mueller)

References

[1] Kidwell MG, Lisch DR. Perspective: transposable elements, parasitic DNA, and genome evolution. Evolution 2001;55:1–24.

[2] Aparicio S, Chapman J, Stupka E, Putnam N, Chia JM, Dehal P, et al. Whole-genome shotgun assembly and analysis of the genome of *Fugu rubripes*. Science 2002;297:1301–10.

[3] Jiao Y, Peluso P, Shi J, Liang T, Stitzer MC, Wang B, et al. Improved maize reference genome with single-molecule technologies. Nature 2017;546:524–7.

[4] McClintock B. The origin and behavior of mutable loci in maize. Proc Natl Acad Sci U S A 1950;36:344–55.

[5] Piegu B, Asgari S, Bideshi D, Federici BA, Bigot Y. Evolutionary relationships of iridoviruses and divergence of ascoviruses from invertebrate iridoviruses in the superfamily Megavirales. Mol Phylogenet Evol 2015;84:44–52.

[6] Jurka J, Kapitonov VV, Pavlicek A, Klonowski P, Kohany O, Walichiewicz J. Repbase Update, a database of eukaryotic repetitive elements. Cytogenet Genome Res 2005;110:462–7.

[7] Wicker T, Sabot F, Hua-Van A, Bennetzen JL, Capy P, Chalhoub B, et al. A unified classification system for eukaryotic transposable elements. Nat Rev Genet 2007;8:973–82.

[8] Finnegan DJ. Eukaryotic transposable elements and genome evolution. Trends Genet 1989;5:103–7.

[9] Goerner-Potvin P, Bourque G. Computational tools to unmask transposable elements. Nat Rev Genet 2018;19:688–704.

[10] Arkhipova IR. Using bioinformatic and phylogenetic approaches to classify transposable elements and understand their complex evolutionary histories. Mob DNA 2017;8:1–14.

[11] Pasquesi GIM, Adams RH, Card DC, Schield DR, Corbin AB, Perry BW, et al. Squamate reptiles challenge paradigms of genomic repeat element evolution set by birds and mammals. Nat Commun 2018;9:1–11.

[12] Jangam D, Feschotte C, Betran E. Transposable element domestication as an adaptation to evolutionary conflicts. Trends Genet 2017;33:817–31.

[13] Sotero-Caio CG, Platt 2nd RN, Suh A, Ray DA. Evolution and diversity of transposable elements in vertebrate genomes. Gen Biol Evol 2017;9:161–77.

[14] Sessions SK, Larson A. Developmental correlates of genome size in plethodontid salamanders and their implications for genome evolution. Evolution 1987;41:1239–51.

[15] Olmo E. Nucleotype and cell size in vertebrates: a review. Basic Appl Histochem 1983;27:227–56.

[16] Szarski H. Cell size and the concept of wasteful and frugal evolutionary strategies. J Theor Biol 1983;105:201–9.

[17] Hanken J, Wake DB. Miniaturization of body size: organismal consequences and evolutionary significance. Ann Rev Ecol Syst 1993;24:501–19.

[18] Roth G, Blanke J, Wake DB. Cell size predicts morphological complexity in the brains of frogs and salamanders. Proc Natl Acad Sci U S A 1994;91:4796–800.

[19] Simonin KA, Roddy AB. Genome downsizing, physiological novelty, and the global dominance of flowering plants. PLoS Biol 2018;16:e2003706.

[20] Gregory TR. Genome size and developmental complexity. Genetica 2002;115:131–46.

[21] Naville M, Henriet S, Warren I, Sumic S, Reeve M, Volff JN, et al. Massive changes of genome size driven by expansions of non-autonomous transposable elements. Curr Biol 2019;29:1161–1168.e6.

[22] Mueller RL. Genome biology and the evolution of cell-size diversity. Cold Spring Harb Perspect Biol 2015;7:a019125.

[23] Lynch M, Conery JS. The origins of genome complexity. Science 2003;302:1401–4.

[24] Mueller RL. piRNAs and evolutionary trajectories in genome size and content. J Mol Evol 2017;85:169–71.

[25] Gregory TR. Animal genome size database Accessed 12 Feb 2018Available from: http://www.genomesize.com, 2019.

[26] Laurin M, Canoville A, Struble M, Organ C, de Buffrenil V. Early genome size increase in urodeles. CR Palevol 2016;15:74–82.

[27] Sun C, Shepard DB, Chong RA, Lopez Arriaza J, Hall K, Castoe TA, et al. LTR retrotransposons contribute to genomic gigantism in plethodontid salamanders. Gen Biol Evol 2012;4:168–83.

[28] Sun C, Lopez Arriaza JR, Mueller RL. Slow DNA loss in the gigantic genomes of salamanders. Gen Biol Evol 2012;4:1340–8.

[29] Elewa A, Wang H, Talavera-Lopez C, Joven A, Brito G, Kumar A, et al. Reading and editing the *Pleurodeles waltl* genome reveals novel features of tetrapod regeneration. Nat Commun 2017;8:1–9.

[30] Nowoshilow S, Schloissnig S, Fei JF, Dahl A, Pang AWC, Pippel M, et al. The axolotl genome and the evolution of key tissue formation regulators. Nature 2018;554:50–5.

[31] Madison-Villar MJ, Sun C, Lau NC, Settles ML, Mueller RL. Small RNAs from a big genome: the piRNA pathway and transposable elements in the salamander species *Desmognathus fuscus*. J Mol Evol 2016;83:126–36.

[32] Sun C, Mueller RL. Hellbender genome sequences shed light on genomic expansion at the base of crown salamanders. Gen Biol Evol 2014;6:1818–29.

[33] Frahry MB, Sun C, Chong R, Mueller RL. Low levels of LTR retrotransposon deletion by ectopic recombination in the gigantic genomes of salamanders. J Mol Evol 2015;80:120–9.

[34] Mueller RL, Jockusch EL. Jumping genomic gigantism. Nat Ecol Evol 2018;2:1687–8.

[35] Liedtke HC, Gower DJ, Wilkinson M, Gomez-Mestre I. Macroevolutionary shift in the size of amphibian genomes and the role of life history and climate. Nat Ecol Evol 2018;2:1792–9.

[36] Edwards RJ, Tuipulotu DE, Amos TG, O'Meally D, Richardson MF, Russell TL, et al. Draft genome assembly of the invasive cane toad, *Rhinella marina*. GigaScience 2018;7:giy095.

[37] Sun YB, Xiong ZJ, Xiang XY, Liu SP, Zhou WW, Tu XL, et al. Whole-genome sequence of the Tibetan frog *Nanorana parkeri* and the comparative evolution of tetrapod genomes. Proc Natl Acad Sci U S A 2015;112:E1257–62.

[38] Rogers RL, Zhou L, Chu C, Marquez R, Corl A, Linderoth T, et al. Genomic takeover by transposable elements in the strawberry poison frog. Mol Biol Evol 2018;35:2913–27.

[39] Hellsten U, Harland RM, Gilchrist MJ, Hendrix D, Jurka J, Kapitonov V, et al. The genome of the Western clawed frog *Xenopus tropicalis*. Science 2010;328:633–6.

[40] Hammond SA, Warren RL, Vandervalk BP, Kucuk E, Khan H, Gibb EA, et al. The North American bullfrog draft genome provides insight into hormonal regulation of long noncoding RNA. Nat Commun 2017;8:1–8.

[41] Li Y, Ren Y, Zhang D, Jiang H, Wang Z, Li X, et al. Chromosome-level assembly of the mustache toad genome using third-generation DNA sequencing and Hi-C analysis. GigaScience 2019;8:giz114.

[42] Genome 10K Community of Scientists. Genome 10K: a proposal to obtain whole-genome sequence for 10,000 vertebrate species. J Hered 2009;100:659–74.

[43] Torres-Sánchez M, Creevey CJ, Kornobis E, Gower DJ, Wilkinson M, San MD. Multi-tissue transcriptomes of caecilian amphibians highlight incomplete knowledge of vertebrate gene families. DNA Res 2018;26:13–20.

[44] Berthelier J, Casse N, Daccord N, Jamilloux V, Saint-Jean B, Carrier G. A transposable element annotation pipeline and expression analysis reveal potentially active elements in the microalga *Tisochrysis lutea*. BMC Genomics 2018;19:1–14.

[45] Hoede C, Arnoux S, Moisset M, Chaumier T, Inizan O, Jamilloux V, et al. PASTEC: an automatic transposable element classification tool. PLoS One 2014;9:e91929.

[46] Tuomisto H. An updated consumer's guide to evenness and related indices. Oikos 2012;8:1203–18.

[47] Venner S, Feschotte C, Biemont C. Dynamics of transposable elements: towards a community ecology of the genome. Trends Genet 2009;25:317–23.

[48] Linquist S, Saylor B, Cottenie K, Elliott TA, Kremer SC, Gregory TR. Distinguishing ecological from evolutionary approaches to transposable elements. Biol Rev 2013;88:573–84.

[49] Linquist S, Cottenie K, Elliott TA, Saylor B, Kremer SC, Gregory TR. Applying ecological models to communities of genetic elements: the case of neutral theory. Mol Ecol 2015;24:3232–42.

[50] Saylor B, Kremer SC, Gregory TR, Cottenie K. Genomic environments and their influence on transposable element communities. bioRxiv 2019;667121.

[51] Simpson EH. Measurement of diversity. Nature 1949;163:688.

[52] Shannon CE. A mathematical theory of communication. Bell Syst Tech J 1948;27:379–423.

[53] Piednoël M, Gonçalves IR, Higuet D, Bonnivard E. Eukaryote DIRS1-like retrotransposons: an overview. BMC Genomics 2011;12:621.

[54] Poulter RTM, Goodwin TJD. DIRS-1 and the other tyrosine recombinase retrotransposons. Cytogenet Genome Res 2005;110:575–88.

[55] Petrov DA, Aminetzach YT, Davis JC, Bensasson D, Hirsh AE. Size matters: non-LTR retrotransposable elements and ectopic recombination in *Drosophila*. Mol Biol Evol 2003;20:880–92.

[56] Bryant DM, Johnson K, DiTommaso T, Tickle T, Couger MB, Payzin-Dogru D, et al. A tissue-mapped axolotl *de novo* transcriptome enables identification of limb regeneration factors. Cell Rep 2017;18:762–76.

[57] Mateo L, Ullastres A, González J. A transposable element insertion confers xenobiotic resistance in *Drosophila*. PLoS Genet 2014;10:e1004560.

[58] Schrader L, Schmitz J. The impact of transposable elements in adaptive evolution. Mol Ecol 2019;28:1537–49.

[59] Keinath MC, Timoshevskiy VA, Timoshevskaya NY, Tsonis PA, Voss SR, Smith JJ. Initial characterization of the large genome of the salamander *Ambystoma mexicanum* using shotgun and laser capture chromosome sequencing. Sci Rep 2015;5:16413.

[60] Zimin AV, Puiu D, Hall R, Kingan S, Clavijo BJ, Salzberg SL. The first near-complete assembly of the hexaploid bread wheat genome, *Triticum aestivum*. GigaScience 2017;6:gix097.

[61] Smith JJ, Timoshevskaya N, Timoshevskiy VA, Keinath MC, Hardy D, Voss SR. A chromosome-scale assembly of the axolotl genome. Genome Res 2019;29:317–24.

[62] Stevens KA, Wegrzyn JL, Zimin A, Puiu D, Crepeau M, Cardeno C, et al. Sequence of the sugar pine megagenome. Genetics 2016;204:1613–26.

[63] Nystedt B, Street NR, Wetterbom A, Zuccolo A, Lin YC, Scofield DG, et al. The Norway spruce genome sequence and conifer genome evolution. Nature 2013;497:579–84.

[64] Neale DB, Wegrzyn JL, Stevens KA, Zimin AV, Puiu D, Crepeau MW, et al. Decoding the massive genome of loblolly pine using haploid DNA and novel assembly strategies. Gen Biol 2014;15:R59.

[65] Kelly LJ, Renny-Byfield S, Pellicer J, Macas J, Novã KP, Neumann P, et al. Analysis of the giant genomes of *Fritillaria* (Liliaceae) indicates that a lack of DNA removal characterizes extreme expansions in genome size. New Phytol 2015;208:596–607.

[66] Weiss-Schneeweiss H, Leitch AR, McCann J, Jang TS, Macas J. Employing next generation sequencing to explore the repeat landscape of the plant genome. In: Hörandl E, Appelhans MS, editors. Next Generation Sequencing in Plant Systematics. Koeltz Scientific Books; 2015, p. 155–79.

[67] Langley CH, Montgomery E, Hudson R, Kaplan N, Charlesworth B. On the role of unequal exchange in the containment of transposable element copy number. Genet Res 1988;52:223–35.

[68] Furano AV, Duvernell DD, Boissinot S. L1 (LINE-1) retrotransposon diversity differs dramatically between mammals and fish. Trends Genet 2004;20:9–14.

[69] Boissinot S, Sookdeo A. The evolution of LINE-1 in vertebrates. Gen Biol Evol 2016;8:3485–507.

[70] Abrusán G, Krambeck HJ. Competition may determine the diversity of transposable elements. Theoret Pop Biol 2006;70:364–75.

[71] Elliott TA, Gregory TR. Do larger genomes contain more diverse transposable elements?. BMC Evol Biol 2015;15:69.

[72] Kijima TE, Innan H. Population genetics and molecular evolution of DNA sequences in transposable elements. I. A simulation framework. Genetics 2013;195:957–67.

[73] Roessler K, Bousios A, Meca E, Gaut BS. Modeling interactions between transposable elements and the plant epigenetic response: a surprising reliance on element retention. Gen Biol Evol 2018;10:803–15.

[74] Price AL, Eskin E, Pevzner PA. Whole-genome analysis of *Alu* repeat elements reveals complex evolutionary history. Genome Res 2004;14:2245–52.

[75] Hillier LW, Miller W, Birney E, Warren W, Hardison RC, Ponting CP, et al. Sequence and comparative analysis of the chicken genome provide unique perspectives on vertebrate evolution. Nature 2004;432:695–716.

[76] Bendall ML, de Mulder M, Iñiguez LP, Lecanda-Sánchez A, Pérez-Losada M, Ostrowski MA, et al. Telescope: characterization of the retrotranscriptome by accurate estimation of transposable element expression. PLoS Comp Biol 2019;15:e1006453.

[77] Coate JE, Doyle JJ. Variation in transcriptome size: are we getting the message?. Chromosoma 2015;124:27–43.

[78] Biscotti MA, Gerdol M, Canapa A, Forconi M, Olmo E, Pallavicini A, et al. The lungfish transcriptome: a glimpse into molecular evolution events at the transition from water to land. Sci Rep 2016;6:21571.

[79] Castoe TA, Hall KT, Guibotsy Mboulas ML, Gu W, de Koning APJ, Fox SE, et al. Discovery of highly divergent repeat landscapes in snake genomes using high-throughput sequencing. Gen Biol Evol 2011;3:641–53.

[80] Ji Y, Marra NJ, DeWoody JA. Comparative analysis of active retrotransposons in the transcriptomes of three species of heteromyid rodents. Gene 2015;562:95–106.

[81] Arseneau JR, Steeves R, Laflamme M. Modified low-salt CTAB extraction of high-quality DNA from contaminant-rich tissues. Mol Ecol Resour 2017;17:686–93.

[82] Bolger AM, Lohse M, Usadel B. Trimmomatic: a flexible trimmer for Illumina sequence data. Bioinformatics 2014;30:2114–20.

[83] Safonova Y, Bankevich A, Pevzner PA. dipSPAdes: assembler for highly polymorphic diploid genomes. J Comput Biol 2015;22:528–45.

[84] Smit AFA, Hubley R, Green P. RepeatMasker Open-4.0. 2013–2015. http://repeatmasker.org/.

[85] Eddy SR. Accelerated profile HMM searches. PLoS Comp Biol 2011;7:e1002195.

[86] Han Y, Wessler SR. MITE-Hunter: a program for discovering miniature inverted-repeat transposable elements from genomic sequences. Nucleic Acids Res 2010;38:e199.

[87] Wenke T, Dobel T, Sorensen TR, Junghans H, Weisshaar B, Schmidt T. Targeted identification of short interspersed nuclear element families shows their widespread existence and extreme heterogeneity in plant genomes. Plant Cell 2011;23:3117–28.

[88] Yang G, Nagel DH, Feschotte C, Hancock CN, Wessler SR. Tuned for transposition: molecular determinants underlying the hyperactivity of a *Stowaway* MITE. Science 2009;325:1391–4.

[89] Ellinghaus D, Kurtz S, Willhoeft U. LTRharvest, an efficient and flexible software for *de novo* detection of LTR retrotransposons. BMC Bioinformatics 2008;9:18.

[90] Rho M, Tang H. MGEScan-non-LTR: computational identification and classification of autonomous non-LTR retrotransposons in eukaryotic genomes. Nucleic Acids Res 2009;37:e143.

[91] Flutre T, Duprat E, Feuillet C, Quesneville H. Considering transposable element diversification in *de novo* annotation approaches. PLoS One 2011;6:e16526.

[92] Price AL, Jones NC, Pevzner PA. *De novo* identification of repeat families in large genomes. Bioinformatics 2005;21:i351–8.

[93] Goubert C, Modolo L, Vieira C, ValienteMoro C, Mavingui P, Boulesteix M. *De novo* assembly and annotation of the Asian tiger mosquito (*Aedes albopictus*) repeatome with dnaPipeTE from raw genomic reads and comparative analysis with the yellow fever mosquito (*Aedes aegypti*). Genome Biol Evol 2015;7:1192–205.

[94] Li W, Jaroszewski L, Godzik A. Clustering of highly homologous sequences to reduce the size of large protein databases. Bioinformatics 2001;17:282–3.

[95] Zhang J, Kobert K, Flouri T, Stamatakis A. PEAR: a fast and accurate Illumina Paired-End reAd mergeR. Bioinformatics 2013;30:614–20.

[96] Kapusta A, Suh A, Feschotte C. Dynamics of genome size evolution in birds and mammals. Proc Natl Acad Sci U S A 2017;114:E1460–9.

[97] Cho J, Benoit M, Catoni M, Drost HG, Brestovitsky A, Oosterbeek M, et al. Sensitive detection of pre-integration intermediates of long terminal repeat retrotransposons in crop plants. Nat Plants 2019;5:26–33.

[98] Langmead B, Salzberg SL. Fast gapped-read alignment with Bowtie 2. Nat Methods 2012;9:357–9.

[99] Grabherr MG, Haas BJ, Yassour M, Levin JZ, Thompson DA, Amit I, et al. Full-length transcriptome assembly from RNA-Seq data without a reference genome. Nat Biotechnol 2011;29:644–52.

[100] Wang Y, Song F, Zhu J, Zhang S, Yang Y, Chen T, et al. GSA: genome sequence archive. Genomics Proteomics Bioinformatics 2017;15:14–8.